ABSTRACT

Lorem ipsum dolor sit amet, consectetuer adipiscing elit. Ut purus elit, vestibulum ut, placerat ac, adipiscing vitae, felis. Curabitur dictum gravida mauris. Nam arcu libero, nonummy eget, consectetuer id, vulputate a, magna. Donec vehicula augue eu neque. Pellentesque habitant morbi tristique senectus et netus et malesuada fames ac turpis egestas. Mauris ut leo. Cras viverra metus rhoncus sem. Nulla et lectus vestibulum urna fringilla ultrices. Phasellus eu tellus sit amet tortor gravida placerat. Integer sapien est, iaculis in, pretium quis, viverra ac, nunc. Praesent eget sem vel leo ultrices bibendum. Aenean faucibus. Morbi dolor nulla, malesuada eu, pulvinar at, mollis ac, nulla. Curabitur auctor semper nulla. Donec varius orci eget risus. Duis nibh mi, congue eu, accumsan eleifend, sagittis quis, diam. Duis eget orci sit amet orci dignissim rutrum.

INTRODUCTION

Lorem ipsum dolor sit amet, consectetuer adipiscing elit. Ut purus elit, vestibulum ut, placerat ac, adipiscing vitae, felis. Curabitur dictum gravida mauris. Nam arcu libero, nonummy eget, consectetuer id, vulputate a, magna. Donec vehicula augue eu neque. Pellentesque habitant morbi tristique senectus et netus et malesuada fames ac turpis egestas. Mauris ut leo. Cras viverra metus rhoncus sem. Nulla et lectus vestibulum urna fringilla ultrices. Phasellus eu tellus sit amet tortor gravida placerat. Integer sapien est, iaculis in, pretium quis, viverra ac, nunc. Praesent eget sem vel leo ultrices bibendum. Aenean faucibus. Morbi dolor nulla, malesuada eu, pulvinar at, mollis ac, nulla. Curabitur auctor semper nulla. Donec varius orci eget risus. Duis nibh mi, congue eu, accumsan eleifend, sagittis quis, diam. Duis eget orci sit amet orci dignissim rutrum.

Nam dui ligula, fringilla a, euismod sodales, sollicitudin vel, wisi. Morbi auctor lorem non justo. Nam lacus libero, pretium at, lobortis vitae, ultricies et, tellus. Donec aliquet, tortor sed accumsan bibendum, erat ligula aliquet magna, vitae ornare odio metus a mi. Morbi ac orci et nisl hendrerit mollis. Suspendisse ut massa. Cras nec ante. Pellentesque a nulla. Cum sociis natoque penatibus et magnis dis parturient montes, nascetur ridiculus mus. Aliquam tincidunt urna. Nulla ullamcorper vestibulum turpis. Pellentesque cursus luctus mauris.

Nulla malesuada porttitor diam. Donec felis erat, congue non, volutpat at, tincidunt tristique, libero. Vivamus viverra fermentum felis. Donec nonummy pellentesque ante. Phasellus adipiscing semper elit. Proin fermentum massa ac quam. Sed diam turpis, molestie vitae, placerat a, molestie nec, leo. Maecenas lacinia. Nam ipsum ligula, eleifend at, accumsan nec, suscipit a, ipsum. Morbi blandit ligula feugiat magna. Nunc eleifend conse-

quat lorem. Sed lacinia nulla vitae enim. Pellentesque tincidunt purus vel magna. Integer non enim. Praesent euismod nunc eu purus. Donec bibendum quam in tellus. Nullam cursus pulvinar lectus. Donec et mi. Nam vulputate metus eu enim. Vestibulum pellentesque felis eu massa.

Quisque ullamcorper placerat ipsum. Cras nibh. Morbi vel justo vitae lacus tincidunt ultrices. Lorem ipsum dolor sit amet, consectetuer adipiscing elit. In hac habitasse platea dictumst. Integer tempus convallis augue. Etiam facilisis. Nunc elementum fermentum wisi. Aenean placerat. Ut imperdiet, enim sed gravida sollicitudin, felis odio placerat quam, ac pulvinar elit purus eget enim. Nunc vitae tortor. Proin tempus nibh sit amet nisl. Vivamus quis tortor vitae risus porta vehicula.

Fusce mauris. Vestibulum luctus nibh at lectus. Sed bibendum, nulla a faucibus semper, leo velit ultricies tellus, ac venenatis arcu wisi vel nisl. Vestibulum diam. Aliquam pellentesque, augue quis sagittis posuere, turpis lacus congue quam, in hendrerit risus eros eget felis. Maecenas eget erat in sapien mattis porttitor. Vestibulum porttitor. Nulla facilisi. Sed a turpis eu lacus commodo facilisis. Morbi fringilla, wisi in dignissim interdum, justo lectus sagittis dui, et vehicula libero dui cursus dui. Mauris tempor ligula sed lacus. Duis cursus enim ut augue. Cras ac magna. Cras nulla. Nulla egestas. Curabitur a leo. Quisque egestas wisi eget nunc. Nam feugiat lacus vel est. Curabitur consectetuer.

METHODOLOGY

Equivalent layer technique for gravity data processing

Let d_i^o be the observed gravity data at the point (x_i, y_i, z_i), $i = 1, ..., N$, of a local Cartesian system with x axis pointing to North, the y axis pointing to East and the z axis pointing

downward. We consider that the gravity data are properly processed so that they represent the difference between the observed gravity (corrected from non-gravitational effects due to the vehicle motion) and the normal gravity, at the same point. This quantity is called *gravity disturbance* (Hofmann-Wellenhof and Moritz, 2005). Several authors have discussed the differences between the gravity anomaly and the gravity disturbance, as well as proposed that the second is more appropriated for geophysical applications. A detailed discussion about this theoretical topic is beyond the scope of our work and we refer the reader to Li and Götze (2001); Fairhead et al. (2003); Hackney and Featherstone (2003); Hinze et al. (2005) and Vajda et al. (2006, 2007, 2008), for example.

In a local coordinate system, the gravity disturbance can be considered as the z - component (or vertical component) of the gravitational attraction exerted by gravity sources. As a consequence, it can be approximated by a linear combination of ...

$$\delta g(x_i, y_i, z_i) = \sum_{j=1}^{N} p_j a_{ij} \,, \tag{1}$$

$$a_{ij} = \frac{G\,(z_0 - z_i)\,10^{-5}}{[(x_i - x_j)^2 + (y_i - y_j)^2 + (z_i - z_0)^2]^{\frac{3}{2}}} \,. \tag{2}$$

$$\mathbf{d}(\mathbf{p}) = \mathbf{A}\mathbf{p} \,, \tag{3}$$

The elements a_{ij} (equation 2) forming the matrix $\mathbf{A}$ (equation 3) are defined in terms of the coordinates x_i, y_i, x_j and y_j, which are associated with the observed data and the equivalent sources. For convenience, we designate these coordinates as *matrix coordinates* and the indices i and j as *matrix indices*.

$$\Psi(\mathbf{p}) = \|\mathbf{d}^o - \mathbf{d}(\mathbf{p})\|_2^2 + \mu \|\mathbf{p}\|_2^2 \,, \tag{4}$$

$$\hat{\mathbf{p}} = \left(\mathbf{A}^\top \mathbf{A} + \mu \mathbf{I}\right)^{-1} \mathbf{A}^\top \mathbf{d}^o \,. \tag{5}$$

Structure of matrix A for regular grids

Consider that the observed data are located on an $N_x \times N_y$ regular grid of points regularly spaced from Δx and Δy along the x and y directions, respectively, on a horizontal plane defined by the constant vertical coordinate $z_1 < z_0$. As a consequence, a given pair of matrix coordinates (x_i, y_i), defined by the matrix index i, $i = 1, \ldots, N = N_x N_y$, is equivalent to a pair of coordinates (x_k, y_l) given by:

$$x_i \equiv x_k = x_1 + [k(i) - 1]\ \Delta x \,, \tag{6}$$

and

$$y_i \equiv y_l = y_1 + [l(i) - 1]\ \Delta y \,, \tag{7}$$

where $k(i)$ and $l(i)$ are integer functions of the matrix index i. These equations can also be used to define the matrix coordinates x_j and y_j associated with the j-th equivalent source, $j = 1, \ldots, N = N_x N_y$. In this case, the integer functions are evaluated by using the index j instead of i. For convenience, we designate x_k and y_l as *grid coordinates* and the indices k and l as *grid indices*, which are computed with the integer functions.

The integer functions assume different forms depending on the orientation of the regular grid of data. Consider the case in which the grid is oriented along the x-axis (Figure 1a). For convenience, we designate these grids as *x-oriented grids*. For them, we have the following

integer functions:

$$i(k,l) = (l-1)\,N_x + k \quad , \tag{8}$$

$$l(i) = \left\lceil \frac{i}{N_x} \right\rceil \tag{9}$$

and

$$k(i) = i - \left\lceil \frac{i}{N_x} \right\rceil N_x + N_x \quad , \tag{10}$$

where $\lceil \cdot \rceil$ denotes the ceiling function (Graham et al., 1994, p. 67). These integer functions are defined in terms of the matrix index i, but they can be defined in the same way by using the index j. Figure 1a illustrates an x-oriented grid defined by $N_x = 4$ and $N_y = 3$. In this example, the matrix coordinates x_7 and y_7, defined by the matrix index $i = 7$ (or $j = 7$), are equivalent to the grid coordinates x_3 and y_2, which are defined by the grid indices $k = 3$ and $l = 2$, respectively. These indices are computed with equations 9 and 10, by using the matrix index $i = 7$ (or $j = 7$).

Now, consider the case in which the regular grid of data is oriented along the y-axis (Figure 1b). For convenience, we call them *y-oriented grids*. Similarly to x-oriented grids, we have the following integer functions associated with y-oriented grids:

$$i(k,l) = (k-1)\,N_y + l \quad , \tag{11}$$

$$k(i) = \left\lceil \frac{i}{N_y} \right\rceil \tag{12}$$

and

$$l(i) = i - \left\lceil \frac{i}{N_y} \right\rceil N_y + N_y \quad . \tag{13}$$

Figure 1b illustrates an y-oriented grid defined by $N_x = 4$ and $N_y = 3$. In this example, the matrix coordinates x_7 and y_7, defined by the matrix index $i = 7$ (or $j = 7$), are equivalent to the grid coordinates x_3 and y_1, which are defined by the grid indices $k = 3$ and $l = 1$,

respectively. Differently from the example shown in Figure 1a, the grid indices of the present example are computed with equations 12 and 13, by using the matrix index $i = 7$ (or $j = 7$).

The element a_{ij} (equation 2) can be rewritten by using equations 6 and 7, giving rise to:

$$a_{ij} = \frac{G\,\Delta z\,10^{-5}}{\left[(\Delta k_{ij}\,\Delta x)^2 + (\Delta l_{ij}\,\Delta y)^2 + (\Delta z)^2\right]^{\frac{3}{2}}}\,, \tag{14}$$

where $\Delta z = z_0 - z_1$, $\Delta k_{ij} = k(i) - k(j)$ (equations 10 and 12) and $\Delta l_{ij} = l(i) - l(j)$ (equations 9 and 13). Notice that the structure of matrix $\mathbf{A}$ (equation 3) for the case in which its elements are given by a_{ij} (equation 14) is defined by the coefficients Δk_{ij} and Δl_{ij}.

For x-oriented grids, the coefficients Δk_{ij} and Δl_{ij} are computed by using equations 10 and 9, respectively. In this case, $\mathbf{A}$ (equation 3) is a symmetric Block-Toeplitz Toeplitz-Block (BTTB) matrix (Chan and Jin, 2007, p. 67) composed of $N_y \times N_y$ blocks, where each block is a symmetric Toeplitz matrix formed by $N_x \times N_x$ elements. For y-oriented grids, the coefficients Δk_{ij} and Δl_{ij} are computed by using equations 12 and 13, respectively. In this case, $\mathbf{A}$ (equation 3) is a symmetric BTTB matrix composed of $N_x \times N_x$ blocks, where each block is a symmetric Toeplitz matrix formed by $N_y \times N_y$ elements. In both cases, the blocks lying at the same diagonal are equal to each other and those located above the main diagonal are equal to those located below. These symmetries come from the fact that the coefficients Δk_{ij} and Δl_{ij} are squared at the denominator of a_{ij} (equation 14).

We follow the common notation found in the literature and represent the blocks of $\mathbf{A}$ as $\mathbf{A}_m$. For x-oriented grids, the index m varies from 0, at the main diagonal, to $N_y - 1$, at the corners of $\mathbf{A}$. In this case, the index m is defined as an integer function of the matrix

indices i and j as follows:

$$m(i,j) = \mid l(i) - l(j) \mid \quad , \tag{15}$$

where $l(i)$ and $l(j)$ are defined by equation 9. The elements forming the first column of $\mathbf{A}_m$ are conveniently represented as a_n^m, $n = 0, \ldots, N_x - 1$, where $m \equiv m(i,j)$ (equation 15) and the subscript index n is defined by the following integer function:

$$n(i,j) = \mid k(i) - k(j) \mid \quad , \tag{16}$$

where $k(i)$ and $k(j)$ are defined by equation 10. For y-oriented grids, the index m varies from 0, at the main diagonal, to $N_x - 1$, at the corners of $\mathbf{A}$. The index m vary from 0, at the main diagonal, to $N_x - 1$, at the corners of $\mathbf{A}$. In such grids, m is given by:

$$m(i,j) = \mid k(i) - k(j) \mid \quad , \tag{17}$$

where the integer functions $k(i)$ and $k(j)$ are defined by equation 12. In this case, the elements forming the first column of $\mathbf{A}_m$ are represented as a_n^m, $n = 0, \ldots, N_y - 1$, where $m \equiv m(i,j)$ (equation 17) and the subscript index n is defined by:

$$n(i,j) = \mid l(i) - l(j) \mid \quad , \tag{18}$$

where $l(i)$ and $l(j)$ are defined by equation 13. For convenience, we designate the indices m and n as *block indices*.

It is important noting that different matrix indices i or j produce the same absolute values for the grid indices k (equations 10 and 12) and l (equations 9 and 13). As a consequence, different pairs of matrix indices i and j generate the same absolute values for the coefficients Δk_{ij} and Δl_{ij} that compose the denominator of a_{ij} (equation 14). It means that elements a_{ij} defined by different matrix indices i and j have the same value. The key point for understanding the structure of matrix $\mathbf{A}$ is then, given a single element a_{ij}

defined by matrix indices i and j, compute the grid indices k (equations 10 and 12) and l (equations 9 and 13). These grid indices are used to (1) compute the coefficients Δk_{ij} and Δl_{ij} and determine the value of a_{ij} with equation 14 and (2) compute the block indices m (equations 15, and 17) and n (equations 16 and and 18) and determine the positions where a_{ij} appears in matrix $\mathbf{A}$.

Consider the x-oriented grid of $N_x \times N_y$ points shown in Figure 1a, with $N_x = 4$, $N_y = 3$ and $N = N_x\, N_y = 12$. This grid results in a matrix $\mathbf{A}$ given by:

$$\mathbf{A} = \begin{bmatrix} \mathbf{A}_0 & \mathbf{A}_1 & \mathbf{A}_2 \\ \mathbf{A}_1 & \mathbf{A}_0 & \mathbf{A}_1 \\ \mathbf{A}_2 & \mathbf{A}_1 & \mathbf{A}_2 \end{bmatrix} \quad , \tag{19}$$

where $\mathbf{A}_m$, $m = 0, 1, 2$, are symmetric Toeplitz matrices given by:

$$\mathbf{A}_m = \begin{bmatrix} a_0^m & a_1^m & a_2^m & a_3^m \\ a_1^m & a_0^m & a_1^m & a_2^m \\ a_2^m & a_1^m & a_0^m & a_1^m \\ a_3^m & a_2^m & a_1^m & a_0^m \end{bmatrix} \quad . \tag{20}$$

To illustrate the relationship between the block indices (m and n) and the matrix indices (i and j), consider the element a_{ij} defined by $i = 2$ and $j = 10$, which is located at the upper right corner of $\mathbf{A}$, in the 2nd line and 10th column. By using equations 9 and 10, we obtain the grid indices $l(i) = 1$, $l(j) = 3$, $k(i) = 2$ and $k(j) = 2$. These grid indices result in the coefficients $\Delta k_{ij} = 0$ and $\Delta l_{ij} = -2$, which are used to compute the element a_{ij} (equation 14), as well as in the block indices $m = 2$ (equation 15) and $n = 0$ (equation 16). These block indices indicate that this element a_{ij} appears in the main diagonal of the blocks $\mathbf{A}_2$, which are located at the corners of $\mathbf{A}$. To verify this, let us take the matrix indices associated with these elements. They are $(i, j) = (1, 9)$, $(2, 10)$, $(3, 11)$, $(4, 12)$, $(9, 1)$, $(10, 2)$,

$(11, 3)$ and $(12, 4)$. By using these matrix indices, it is easy to verify that all of them produce the same grid indices $l(i)$, $l(j)$, $k(i)$ and $k(j)$ (equations 9 and 10) as those associated with the element defined by $i = 2$ and $j = 10$. Consequently, all of them produce elements a_{ij} (equation 14) having the same value. Besides, it is also easy to verify that all these matrix indices produce the same block indices $m = 2$ (equation 15) and $n = 0$ (equation 16). By repeating this procedure for all elements a_{ij}, $i = 0, 1, 2, 3$, $j = 0, 1, 2$, forming the matrix $\mathbf{A}$ obtained from our x-oriented grid (Figure 1a), we can verify the well-defined pattern represented by equations 19 and 20. This procedure can also be used to verify that the matrix $\mathbf{A}$ obtained from the y-oriented grid illustrated in Figure 1b is given by

$$\mathbf{A} = \begin{bmatrix} \mathbf{A}_0 & \mathbf{A}_1 & \mathbf{A}_2 & \mathbf{A}_3 \\ \mathbf{A}_1 & \mathbf{A}_0 & \mathbf{A}_1 & \mathbf{A}_2 \\ \mathbf{A}_2 & \mathbf{A}_1 & \mathbf{A}_2 & \mathbf{A}_1 \\ \mathbf{A}_3 & \mathbf{A}_2 & \mathbf{A}_1 & \mathbf{A}_0 \end{bmatrix} \quad , \tag{21}$$

where $\mathbf{A}_m$, $m = 0, 1, 2, 3$, are symmetric Toeplitz matrices given by:

$$\mathbf{A}_m = \begin{bmatrix} a_0^m & a_1^m & a_2^m \\ a_1^m & a_0^m & a_1^m \\ a_2^m & a_1^m & a_0^m \end{bmatrix} \quad . \tag{22}$$

Computational performance

In a normal procedure of the fast equivalent layer proposed by Siqueira et al. (2017), at each iteration a full matrix $\mathbf{A}$ (equation 3) is multiplied by the estimated mass distribution parameter vector $\hat{\mathbf{p}}^k$ producing the predicted gravity data $\mathbf{d}(\mathbf{p})$ iteratively . As pointed in Siqueira et al. (2017) the number of flops (floating-point operations) necessary to estimate the N-dimensional parameter vector inside the iteration loop is:

$$f_0 = N^{it}(3N + 2N^2) \ , \tag{23}$$

where N^{it} is the number of iterations. From equation 23 it is clear that the matrix-vector product ($2N^2$) accounts for most of the computational complexity in this method.

It is well known that FFT takes $N \log_2(N)$ flops (**?**). Computing the eigenvalues of the BCCB matrix ($4N \times 4N$) and applying 2D-FFT on the parameter vector (equation **??**), takes $4N \log(4N)$ each. The point-multiplication takes $4N$. As it is necessary to compute the inverse FFT another two $4N \log(4N)$ must be taken in account. However, the sensibility matrix does not change during the process, thus, the eigenvalues of BCCB must be calculated only once, outside of the iteration. This lead us to a flops count in our method of:

$$f_1 = 4N \log(4N) + N^{it}(7N + 8N \log(4N)). \tag{24}$$

Another major improvement of this methodology is the exoneration of calculating the full sensibility matrix $\mathbf{A}$ (equation 3). Each element needs 12 flops (equation 2), totalizing $12N^2$ flops for the full matrix. Calculating only the first row of the BTTB matrix $12N$ flops is required. Thus, the full flops count of the method presented by Siqueira et al. (2017):

$$f_s = 12N^2 + N^{it}(3N + 2N^2), \tag{25}$$

it is decreased in our method to:

$$f_f = 12N + 4N \log(4N) + N^{it}(7N + 8N \log(4N)). \tag{26}$$

Figure 1 shows the floating points to estimate the parameter vector using the fast equivalent layer with the method of Siqueira et al. (2017) (equation 23) and our approach (equation 24) versus the number of observation points varyig from $N = 5000$ to $N = 1000000$ with 50 iterations. The number of operations is drastically decreased.

Table 1 shows the system memory RAM usage needed to store the full sensibility matrix, the BTTB first row and the BCCB eigenvalues (8 times the BTTB first row). The quantities were computed for different numbers of data (N) with the same corresponding number of equivalent sources (N). Table 1 considers that each element of the matrix is a double-precision number, which requires 8 bytes of storage, except for the BCCB complex eigenvalues, which requires 16 bytes per element. Notice that $1,000.000$ observation points requires nearly 7.6 Terabytes of memory RAM to store the whole sensibility matrix of the equivalent layer.

Using a PC with a Intel Core i7 4790@3.6GHz processor and 16 Gb of memory RAM, Figure 2 compares the running time of the Siqueira et al. (2017) method with the one of our work, considering a constant number of iterations equal to 50. Clearly, the major advantage of our approach is its computational efficiency that allows a rapid calculation of the gravity forward modeling with number of observations greater than $10,000$. Because of the RAM available in this system, we could not perform this comparison with more observations. Therefore, the number of observation is limited to $22,500$. Disregarding the limitation of 16 Gb of RAM, Figure 3 shows the running time of our method with 50 iterations and with the number of observations up to 25 millions. Our method requires $26 : 8$ seconds to run one million of observations, whereas Siqueira et al. (2017) method took $48 : 3$ seconds to run $22,500$ observations

SYNTHETIC TESTS

In this section, we investigate the effectiveness of using the properties of BTTB and BCCB matrices (equation **??**) to solve, at each iteration, the forward modeling (the matrix-vector product $\mathbf{A}\hat{\mathbf{p}}^k$) required in the fast equivalent layer proposed by Siqueira et al. (2017). We simulated three sources whose horizontal projections are shown in Figure 4 as black lines. These sources are two vertical prisms with density contrasts of $0.35g/cm^3$ (upper-left prism) and $0.4g/cm^3$ (upper-right prism) and a sphere with radius of 1,000 m with density contrast of $-0.5g/cm^3$. Figure 4 shows the vertical component of gravity field generated by these sources contaminated with additive pseudorandom Gaussian noise with zero mean and standard deviation of 0.01486 mGal.

The advantage of using the structures of BTTB and BCCB matrices to compute forward modeling in the fast equivalent layer proposed by Siqueira et al. (2017) is grounded on the use of regular grids of data and equivalent sources. Hence, we created 10,000 observation points regularly spaced in a grid of 100×100 at 100 m height. We also set a grid of equivalent point masses, each one directly beneath each observation points, located at 300 m deep. Figures 5a and 6a show the fitted gravity data obtained, respectively, by the fast equivalent layer using Siqueira et al. (2017) method and by our modified form of this method that computes the forward modeling using equation **??**. The corresponding residuals (Figures 5b and 6b), defined as the difference between the observed (Figure 4) and fitted gravity data (Figures 5a and 6a), show means close to zero and standard deviations of 0.0144 mGal. Therefore, Figures 5 and 6 show that Siqueira et al. (2017) method and our modified version of this method produced virtually the same results. This excellent agreement is confirmed in Figures 7 and 8 which shows that there are virtually no differences, respectively, in the

fitted data presented in Figures 5b and 6b and in the estimated mass distributions within the equivalent layers (not shown) yielded by both Siqueira et al. (2017) method and our modification of this method. These results (7 and 8) show that computing the matrix-vector product ($\mathbf{A}\hat{\mathbf{p}}^k$), required in the forward modeling, by means of embedding the BTTB matrix into a BCCB matrix (equation **??**) yields practically the same result as the one produced by computing this matrix-vector product with a full matrix $\mathbf{A}$.

We perform two forms of processing the gravity data (Figure 4) through the equivalent layer technique: the upward (Figure 9) and the downward (Figure 10) continuations. The upward height is 300m and the downward is at 50m. Either in the upward continuation (Figure 9) or in the downward continuation (Figure 10), the continued gravity data using the fast equivalent layer proposed by Siqueira et al. (2017) (Figures 9a and 10a) are in close agreement with those produced by our modification of Siqueira et al. (2017) method (Figures 9b and 10b). The residuals (Figures 9c and 10c) quantify this agreement since their means and standard deviations are close to zero in both continued gravity data using both methods. All the continued gravity data shown here (Figures 9 and 10) agree with the true ones (not shown). The most striking feature of these upward or the downward continuations concerns the total computation time. The computation time spent by our method is approximately 1500 times faster than Siqueira et al. (2017) method.

REAL DATA TEST

Test with real data are conducted with the gravity data from Carajás, north of Brazil, were provided by the Geological Survey of Brazil (CPRM). The real aerogravimetric data were collected in 113 flight lines along northsouth direction with flight line spacing of 3 km and tie lines along eastwest direction at 12 km.

This airborne gravity survey was divided in two different areas, collected in different times, having samples spacing of 7.65 m and 15.21 m, totalizing 4,353,428 observation points. The height of the flight was fixed at 900 m. The gravity data (Figure 11) were gridded into a regularly spaced dataset of $250,000$ observation points (500×500) with a grid spacing of 716.9311 km north-south and 781.7387 km east-west.

To apply our modification of the fast equivalent layer method (Siqueira et al., 2017) that computes the forward modeling using the properties of BTTB and BCCB matrices (equation **??**), we set an equivalent layer at 300 m deep. Figure 12a shows the fitted gravity data after with 50 iterations by applying our method approach. The residuals (Figure 12b), defined as the difference between the observed (Figure 11) and the predicted (Figure 12a) data, show an acceptable data fitting because they have a mean close to zero (0.000292 mGal) and a small standard deviation of 0.105 mGal which corresponds to approximately 0.1 % of the amplitude of the gravity data.

These small residuals indicate that our method yielded an estimated mass distribution (not shown) that can be used in the data processing. We perform upward-continuation of the real gravity data (Figure 11) at a constant height of 5000 m over the real data. The upward-continued gravity data (Figure 13) seem a reasonable processing because of the attenuatinon of the short-wave lenghts. By using our approach, the processing of the 250,000 observations was extremely fast and took 0.216 seconds.

CONCLUSIONS

By exploring the properties related to Block-Toeplitz Toeplitz-block (BTTB) and Block-Circulant Circulant-Block (BCCB) matrices in the gravity data processing, we have pro-

posed a new efficient approach for calculating the gravity-data forward modeling required in the iterative fast equivalent-layer technique grounded on excess mass constraint that does not demand the solution of linear systems. Its efficiency is grounded on the use of regular grids of observations and equivalent sources (point masses). Our algorithm greatly reduces the number of flops necessary to estimate a 2D mass distribution within the equivalent layer that fits the observed gravity data. For example, when processing one million observations the number of flops is reduced in 104 times. Traditionally, such amount of data impractically requires 7.6 Terabytes of RAM memory to handle the full sensibility matrix. Rather, in our method, this matrix takes 61,035 Megabytes of RAM memory only.

Our method takes advantage of the symmetric BTTB system that arises when processing a harmonic function as the vertical component of gravity, that depends on the inverse of distance between the observation and the point mass over the equivalent layer. Symmetric BTTB matrices can be stored by its only first row and can be embedded into a symmetric BCCB matrix, which in turn also only needs its first row.

Using the fast Fourier transform it is possible to calculate the eigenvalues of BCCB matrices which can be used to compute a matrix-vector product (gravity-data forward modeling) in a very low computational cost. The time needed to process medium-sized grids of observation, for example 22,500 points, is reduced in 102 times. We have successfully applied the proposed method to upward (or downward) synthetic gravity data. Testing on field data from the Carajás Province, north of Brazil, confirms the potential of our approach in upward-continuing gravity data with 250,000 observations in about 0.2 seconds. Our method allows, in future research, applying the equivalent layer technique for processing and interpreting massive data set such as collected in continental and global scales studies.

Figures

Figure 1

Figure 2

Figure 3

Figure 4

Figure 5

Figure 6

Figure 7

Figure 8

Figure 9

Figure 10

Figure 11

Figure 12

Figure 13

Tables

$N \times N$	**Full RAM (Mb)**	**BTTB RAM (Mb)**	**BCCB RAM (Mb)**
100×100	0.0763	0.0000763	0.0006104
400×400	1.22	0.0031	0.0248
2500×2500	48	0.0191	0.1528
10000×10000	763	0.00763	0.6104
40000×40000	12207	0.305	2.4416
250000×250000	476837	1.907	15.3
500000×500000	1907349	3.815	30.518
1000000×1000000	7629395	7.629	61.035

Table 1: Comparison between the system memory RAM usage needed to store the full matrix, the BTTB first row and the BCCB eigenvalues (eight times the BTTB). The quantities were computed for different numbers of data (N) with the same corresponding number of equivalent sources (N). This table considers that each element of the matrix is a double-precision number, which requires 8 bytes of storage, except for the BCCB complex eigenvalues, which requires 16 bytes per element.

ACKNOWLEDGMENTS

This study was financed by the brazilian agencies CAPES (in the form of a scholarship), FAPERJ (grant n.° E-26 202.729/2018) and CNPq (grant n.° 308945/2017-4).

REFERENCES

Chan, R. H.-F., and X.-Q. Jin, 2007, An introduction to iterative toeplitz solvers: SIAM, **5**.

Fairhead, J. D., C. M. Green, and D. Blitzkow, 2003, The use of gps in gravity surveys: The Leading Edge, **22**, 954–959.

Golub, G. H., and C. F. V. Loan, 2013, Matrix computations (johns hopkins studies in the mathematical sciences), 4 ed.: Johns Hopkins University Press.

Graham, L., D. E. Knuth, and O. Patashnik, 1994, Concrete mathematics: a foundation for computer science, 2 ed.: Addison-Wesley Publishing Company.

Hackney, R. I., and W. E. Featherstone, 2003, Geodetic versus geophysical perspectives of the gravity anomaly: Geophysical Journal International, **154**, 35–43.

Hinze, W. J., C. Aiken, J. Brozena, B. Coakley, D. Dater, G. Flanagan, R. Forsberg, T. Hildenbrand, G. R. Keller, J. Kellogg, R. Kucks, X. Li, A. Mainville, R. Morin, M. Pilkington, D. Plouff, D. Ravat, D. Roman, J. Urrutia-Fucugauchi, M. Véronneau, M. Webring, and D. Winester, 2005, New standards for reducing gravity data: The north american gravity database: GEOPHYSICS, **70**, J25–J32.

Hofmann-Wellenhof, B., and H. Moritz, 2005, Physical geodesy: Springer.

Li, X., and H.-J. Götze, 2001, Ellipsoid, geoid, gravity, geodesy, and geophysics: Geophysics, **66**, 1660–1668.

Siqueira, F. C., V. C. Oliveira Jr, and V. C. Barbosa, 2017, Fast iterative equivalent-layer technique for gravity data processing: A method grounded on excess mass constraint: Geophysics, **82**, G57–G69.

Vajda, P., A. Ellmann, B. Meurers, P. Vaníček, P. Novák, and R. Tenzer, 2008, Global ellipsoid-referenced topographic, bathymetric and stripping corrections to gravity distur-

bance: Studia Geophysica et Geodaetica, **52**, 19.

Vajda, P., P. Vaníček, and B. Meurers, 2006, A new physical foundation for anomalous gravity: Studia Geophysica et Geodaetica, **50**, 189–216.

Vajda, P., P. Vaníček, P. Novák, R. Tenzer, and A. Ellmann, 2007, Secondary indirect effects in gravity anomaly data inversion or interpretation: Journal of Geophysical Research: Solid Earth, **112**.

LIST OF FIGURES

of 0.0144 mGal.

6 (a) Fitted gravity data produced by our modification of the fast equivalent layer proposed by Siqueira et al. (2017). (b) Gravity residuals, defined as the difference between the observed data in Figure 4 and the predicted data in (a), with their mean of $8.264e-7$ and standard deviation of 0.0144 mGal.

7 Difference between the fitted gravity data produced by Siqueira et al. (2017) method (Figure 5a) and by our modified form of this method that computes the forward modeling using the properties of BTTB and BCCB matrices (equation **??**).

8 Difference between the estimated mass distribution within the equivalent layer produced by Siqueira et al. (2017) method (Figure 5a) and by our modified form of this method that computes the forward modeling using the properties of BTTB and BCCB matrices (equation **??**).

9 The upward-continued gravity data using: (a) the fast equivalent layer proposed by Siqueira et al. (2017) and (b) our modified form of Siqueira et al. (2017) method by using the properties of BTTB and BCCB matrices (equation **??**) to calculate the forward modeling. (c) Residuals, defined as the difference between a and b with their mean of $-5.938e-18$ and standard deviation of $8.701e-18$. The total computation times in the Siqueira et al. (2017) method and in our approach are 7.62026 and 0.00834 seconds, respectively.

10 The downward-continued gravity data using: (a) the fast equivalent layer proposed by Siqueira et al. (2017) and (b) our modified form of Siqueira et al. (2017) method by using the properties of BTTB and BCCB matrices (equation **??**) to calculate the forward modeling. (c) Residuals, defined as the difference between a and b with their mean of $5.914e-18$ and standard deviation of $9.014e-18$. The total computation times in the Siqueira et al. (2017) method and in our approach are 7.59654 and 0.00547 seconds, respectively.

11 Carajás Province, Brazil. Gravity data on a regular grid of 500×500 points, totaling $250,000$ observations. The inset shows the study area (blue rectangle) which covers the southeast part of the state of Pará, north of Brazil.

12 Carajás Province, Brazil. (a) Predicted gravity data produced by our modification of the fast equivalent layer method (Siqueira et al., 2017) that computes the forward modeling using the properties of BTTB and BCCB matrices (equation **??**). (b) Gravity residuals, defined as the difference between the observed data in Figure 11 and the predicted data in a, with their mean of 0.000292 mGal and standard deviation of 0.105 mGal.

13 Carajás Province, Brazil. The upward-continued gravity data using our modification of the fast equivalent layer method (Siqueira et al., 2017) that computes the forward modeling using the properties of BTTB and BCCB matrices (equation **??**). The total computation time is 0.216 seconds for processing of the $250,000$ observations.

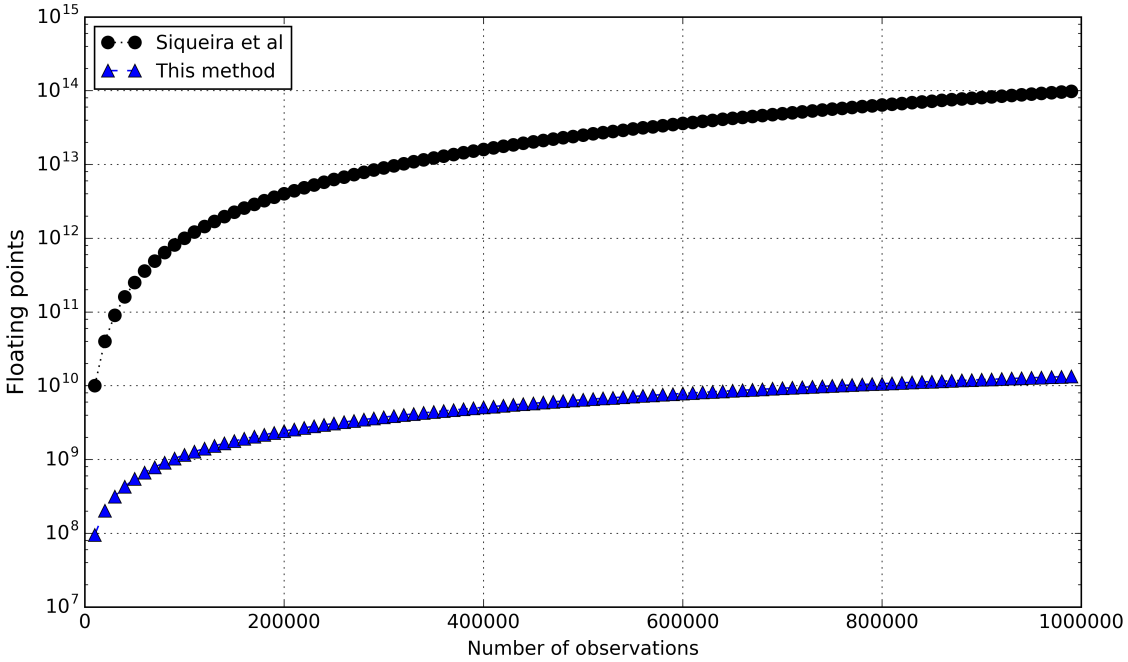

Figure 1: floating points to estimate the parameter vector using the fast equivalent layer with Siqueira et al. (2017) method (equation 23) and our approach (equation 24) versus the numbers of observation points varyig from $N = 5000$ to $N = 1000000$ with 50 iterations. The number of operations is drastically decreased.

– **GEO-XXXX**

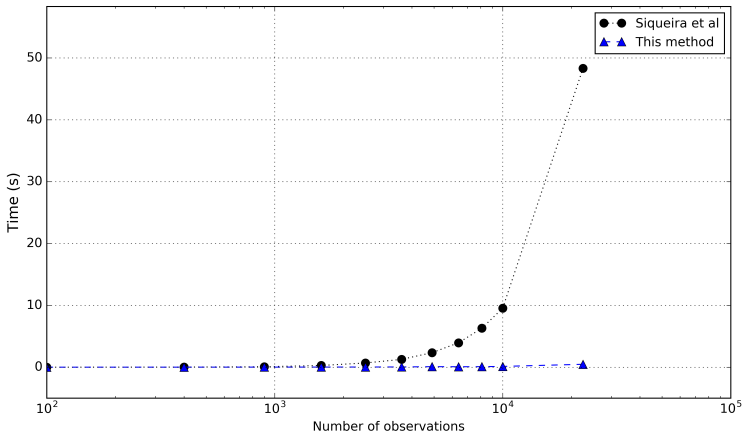

Figure 2: time necessary to run 50 iterations of the Siqueira et al. (2017) method and the one presented in this work. With the limitation of 16 Gb of memory RAM in our system, we could test only up to 22500 obervation points.

– **GEO-XXXX**

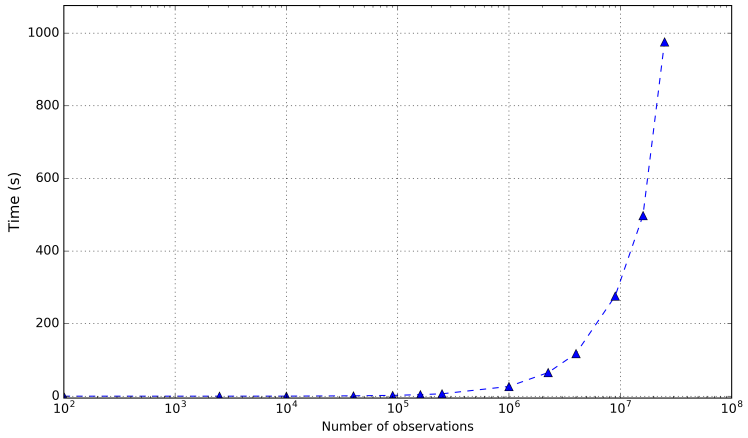

Figure 3: time necessary to run the equivalent layer technique with 50 iterations using only this new approach, where the RAM is not a limitation factor. We could run up to 25 million observation points. In comparison, 1 million observation points took 26.8 seconds to run, where the maximun 22500 observation points in figure 2, with Siqueira et al. (2017) method, took 48.3 seconds.

– **GEO-XXXX**

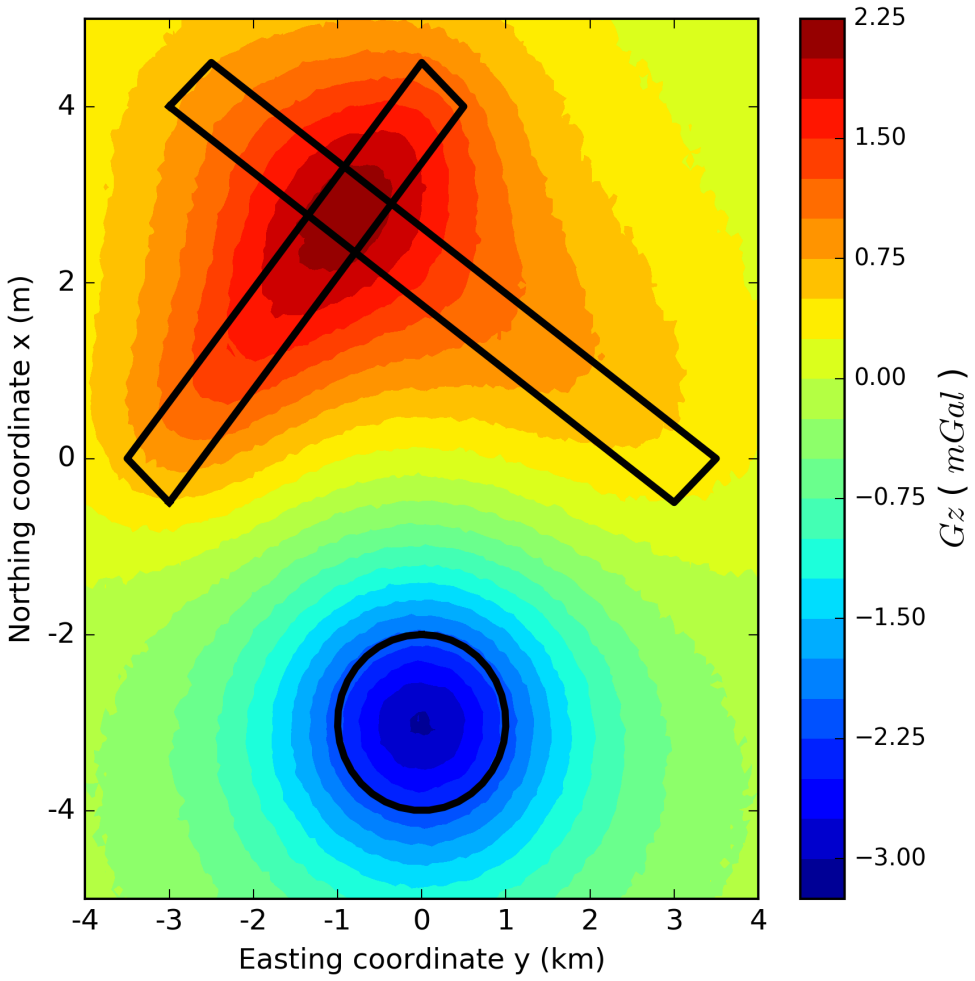

Figure 4: model with two polygonal prisms, with density contrast of 0.35 (upper-left body) and $0.4g/cm^3$ (upper-right body), and a sphere with radius of $1000m$ with density contrast of $-0.5g/cm^3$. The vertical component of gravity generated by this bodies were calculated and are shown together with their horizontal projections. A gaussian noise was added to the data with mean of zero and maximum value of 0.5% of the maximum of the original data. As previous said only in regular grids the BTTB matrix structures appears. We created 10000 observation points regularly spaced in a grid of 100×100, with a uniform $100m$ of height for all the observations.

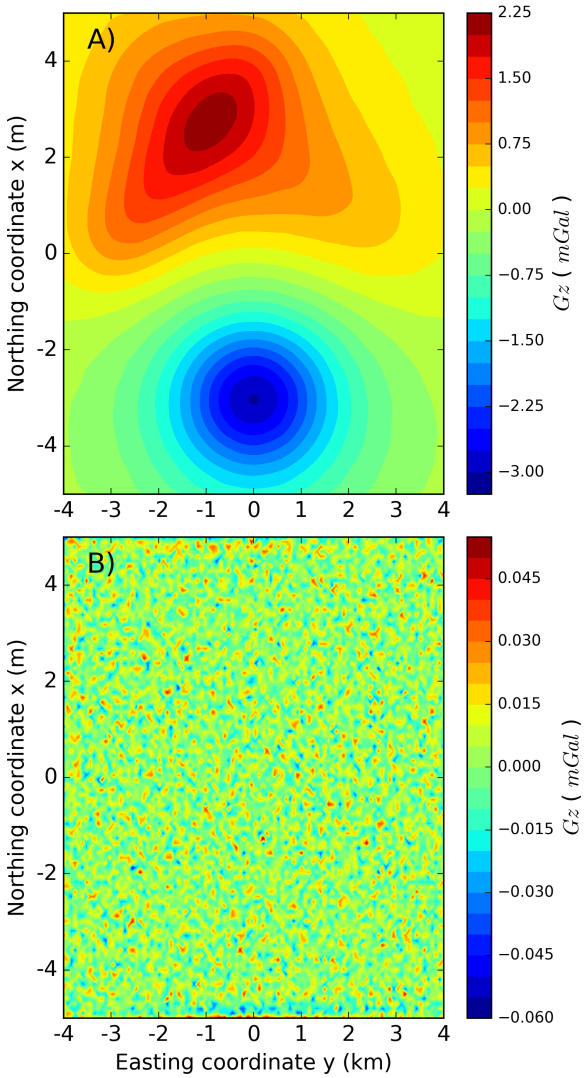

Figure 5: (a) Fitted gravity data produced by the fast equivalent layer proposed by Siqueira et al. (2017). (b) Gravity residuals, defined as the difference between the observed data in Figure 4 and the predicted data in (a), with their mean of $8.264e-7$ and standard deviation of 0.0144 mGal.

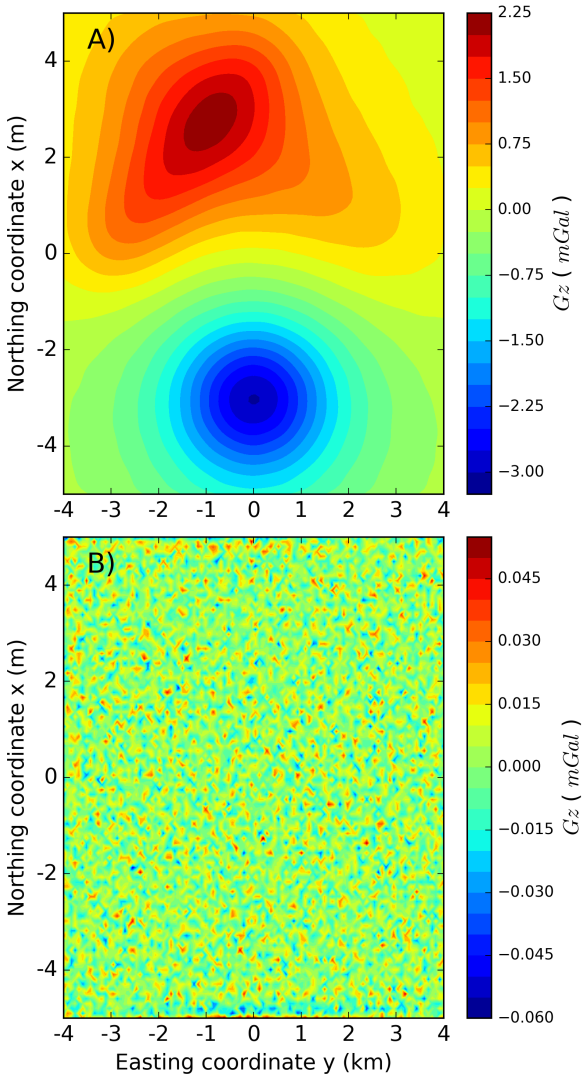

Figure 6: (a) Fitted gravity data produced by our modification of the fast equivalent layer proposed by Siqueira et al. (2017). (b) Gravity residuals, defined as the difference between the observed data in Figure 4 and the predicted data in (a), with their mean of $8.264e-7$ and standard deviation of 0.0144 mGal.

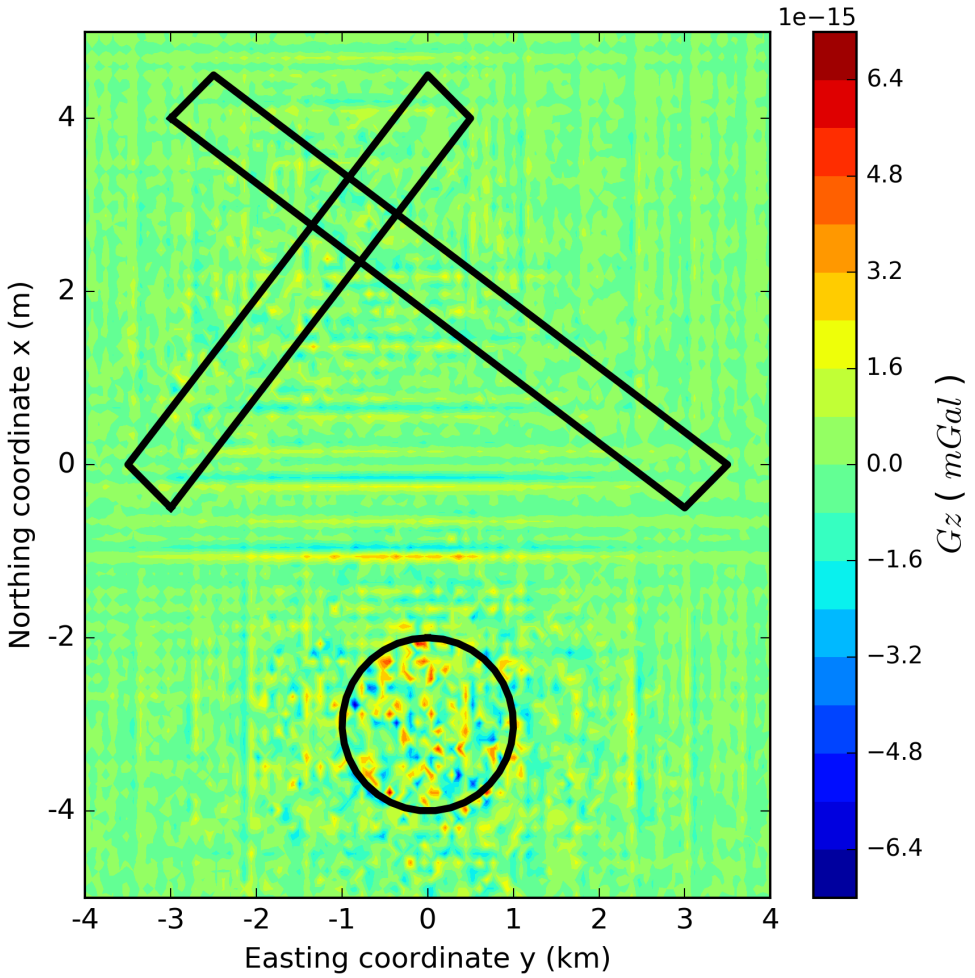

Figure 7: Difference between the fitted gravity data produced by Siqueira et al. (2017) method (Figure 5a) and by our modified form of this method that computes the forward modeling using the properties of BTTB and BCCB matrices (equation **??**).

– **GEO-XXXX**

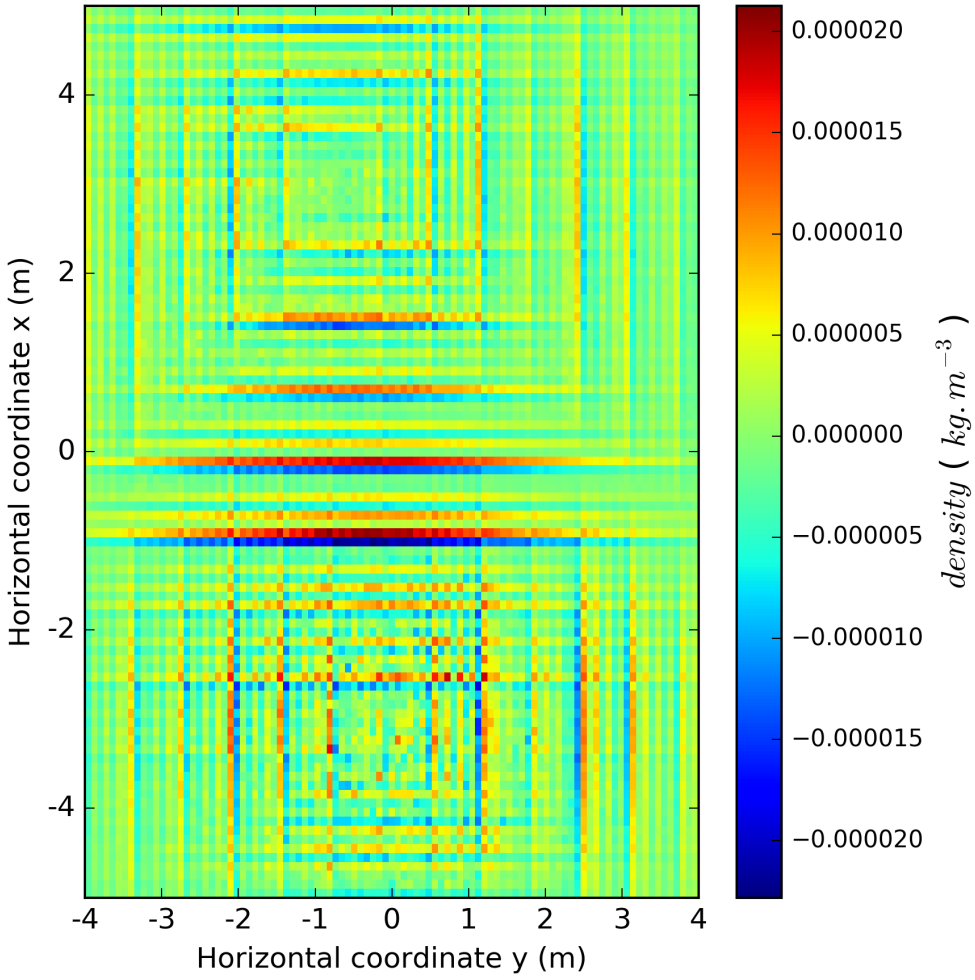

Figure 8: Difference between the estimated mass distribution within the equivalent layer produced by Siqueira et al. (2017) method (Figure 5a) and by our modified form of this method that computes the forward modeling using the properties of BTTB and BCCB matrices (equation **??**).

– **GEO-XXXX**

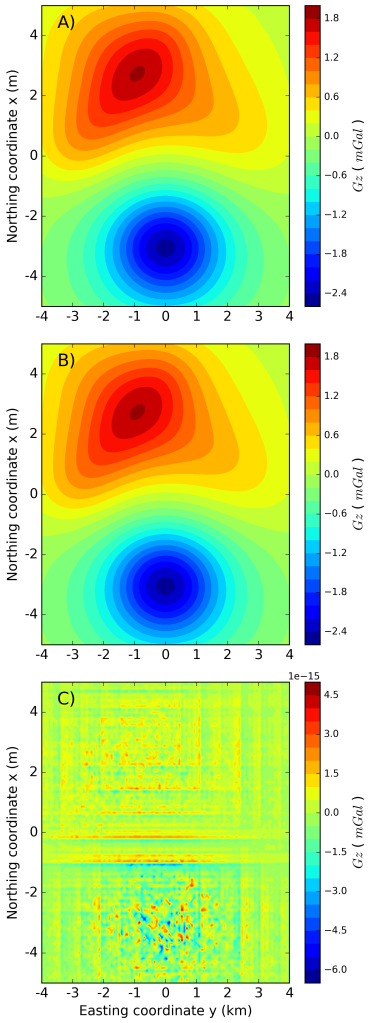

Figure 9: The upward-continued gravity data using: (a) the fast equivalent layer proposed by Siqueira et al. (2017) and (b) our modified form of Siqueira et al. (2017) method by using the properties of BTTB and BCCB matrices (equation **??**) to calculate the forward modeling. (c) Residuals, defined as the difference between a and b with their mean of $-5.938e-18$ and standard deviation of $8.701e-18$. The total computation times in the Siqueira et al. (2017) method and in our approach are 7.62026 and 0.00834 seconds, respectively.

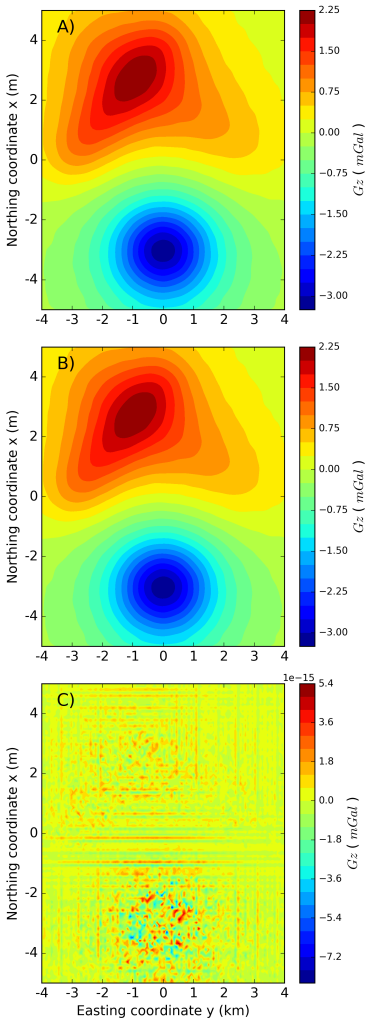

Figure 10: The downward-continued gravity data using: (a) the fast equivalent layer proposed by Siqueira et al. (2017) and (b) our modified form of Siqueira et al. (2017) method by using the properties of BTTB and BCCB matrices (equation **??**) to calculate the forward modeling. (c) Residuals, defined as the difference between a and b with their mean of $5.914e-18$ and standard deviation of $9.014e-18$. The total computation times in the Siqueira et al. (2017) method and in our approach are 7.59654 and 0.00547 seconds, respectively.

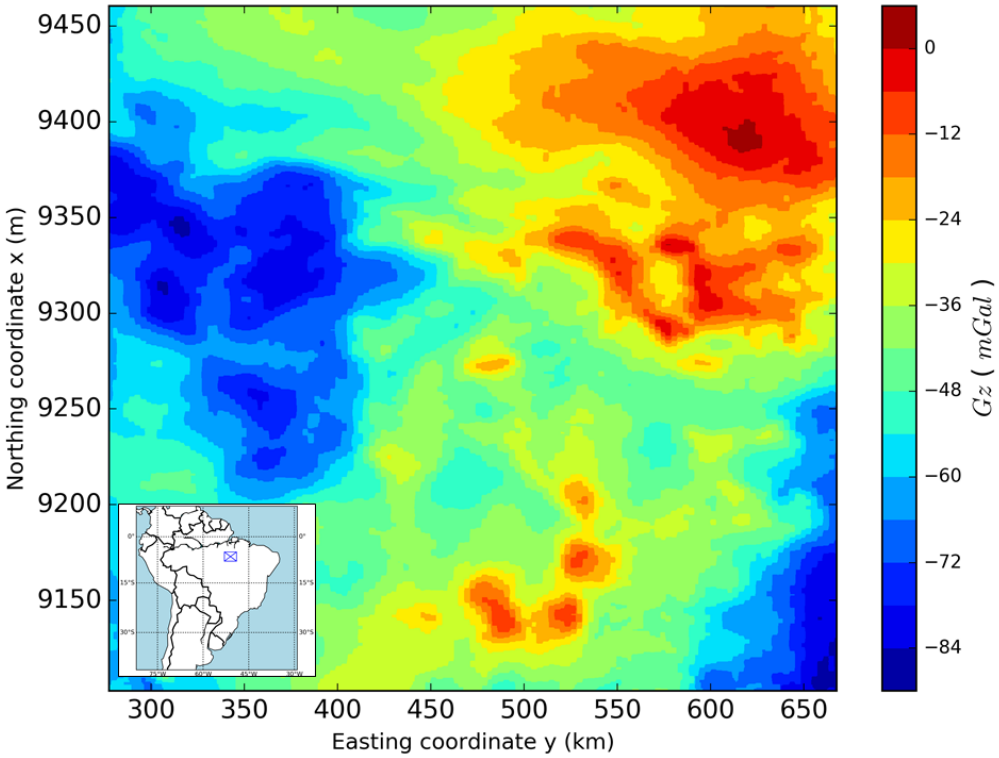

Figure 11: Carajás Province, Brazil. Gravity data on a regular grid of 500×500 points, totaling $250,000$ observations. The inset shows the study area (blue rectangle) which covers the southeast part of the state of Pará, north of Brazil.

– **GEO-XXXX**

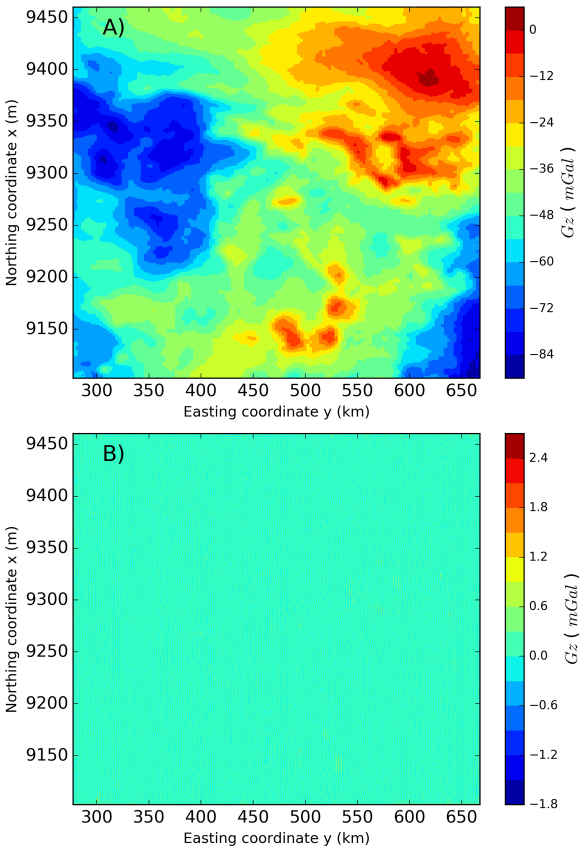

Figure 12: Carajás Province, Brazil. (a) Predicted gravity data produced by our modification of the fast equivalent layer method (Siqueira et al., 2017) that computes the forward modeling using the properties of BTTB and BCCB matrices (equation **??**). (b) Gravity residuals, defined as the difference between the observed data in Figure 11 and the predicted data in a, with their mean of 0.000292 mGal and standard deviation of 0.105 mGal.

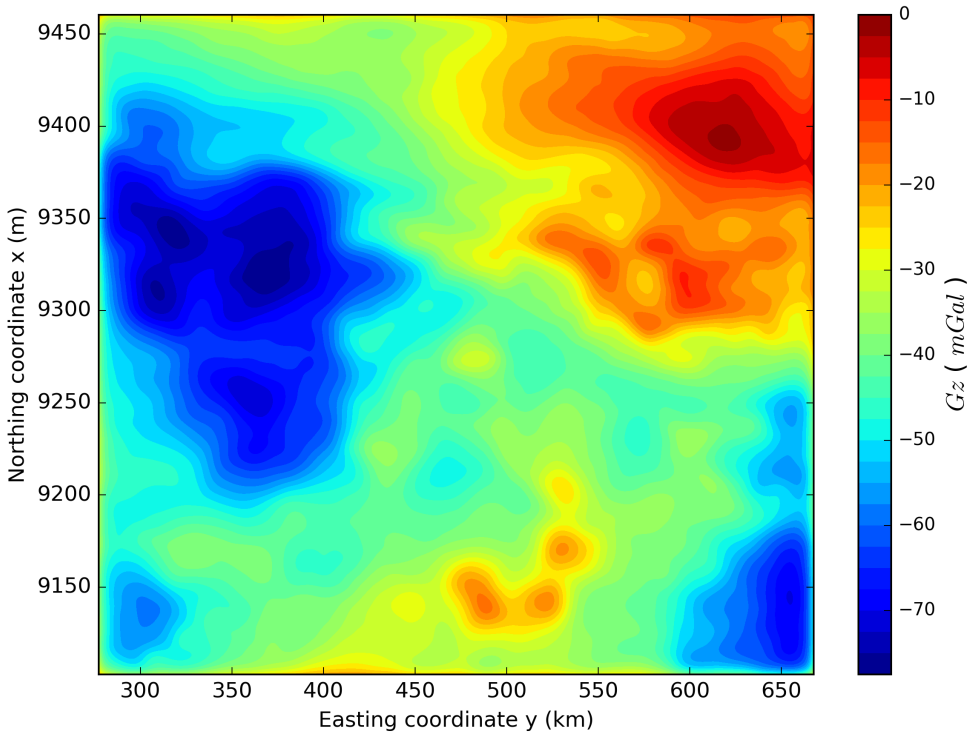

Figure 13: Carajás Province, Brazil. The upward-continued gravity data using our modification of the fast equivalent layer method (Siqueira et al., 2017) that computes the forward modeling using the properties of BTTB and BCCB matrices (equation **??**). The total computation time is 0.216 seconds for processing of the $250,000$ observations.

– **GEO-XXXX**